
EFFICIENT BAYESIAN POLICY REUSE WITH A SCALABLE OBSERVATION MODEL IN DEEP REINFORCEMENT LEARNING

A PREPRINT

Jinmei Liu¹

Zhi Wang¹

Chunlin Chen¹

Daoyi Dong²

¹ Department of Control and Systems Engineering, Nanjing University, Nanjing, China

² School of Engineering and Information Technology, University of New South Wales, Canberra, Australia
mg20150005@smail.nju.edu.cn, {zhiwang, clchen}@nju.edu.cn, daoyidong@gmail.com

ABSTRACT

Bayesian policy reuse (BPR) is a general policy transfer framework for selecting a source policy from an offline library by inferring the task belief based on some observation signals and a trained observation model. In this paper, we propose an improved BPR method to achieve more efficient policy transfer in deep reinforcement learning (DRL). First, most BPR algorithms use the episodic return as the observation signal that contains limited information and cannot be obtained until the end of an episode. Instead, we employ the state transition sample, which is informative and instantaneous, as the observation signal for faster and more accurate task inference. Second, BPR algorithms usually require numerous samples to estimate the probability distribution of the tabular-based observation model, which may be expensive and even infeasible to learn and maintain, especially when using the state transition sample as the signal. Hence, we propose a scalable observation model based on fitting state transition functions of source tasks from only a small number of samples, which can generalize to any signals observed in the target task. Moreover, we extend the offline-mode BPR to the continual learning setting by expanding the scalable observation model in a plug-and-play fashion, which can avoid negative transfer when faced with new unknown tasks. Experimental results show that our method can consistently facilitate faster and more efficient policy transfer.

Keywords Bayesian policy reuse, continual learning, deep reinforcement learning, observation model, transfer learning.

1 Introduction

Reinforcement learning (RL) [1] is a general optimization framework of how an artificial agent learns an optimal policy to maximize the cumulative reward by interacting with its environment. With recent advances, deep RL (DRL) has achieved state-of-the-art performance on various tasks [2, 3], such as video games [4], board games [5], robotics [6], autonomous driving [7], and quantum information [8]. However, DRL algorithms are sensitive to the choice of hyperparameters [9, 10] and typically require numerous samples to converge to good policies [11, 12], which can be computationally intensive in real-world applications.

To address this concern, transfer RL [13] is usually introduced to reduce the number of samples required for learning a target task by reusing previously acquired knowledge from relevant source tasks [14–16]. Reusing policies is a widely investigated kind of approaches in this topic [17–21], since it is intuitive, direct, and does not rely on value functions that may be difficult or unavailable to transfer.

In this paper, we focus on the problem of transferring policies from multiple source tasks in DRL. Bayesian policy reuse (BPR) [22] is a general transfer framework for responding to a target task by selecting the most appropriate policy from an offline library based on some observation signals and a trained observation model. Moreover, BPR has been successfully applied to handle non-stationary opponents in multi-agent systems [23–26]. However, BPR algorithms have several limitations: 1) they usually use the episodic return as the observation signal that is only a

scalar containing limited information, and the learning can be too slow as they must wait until the end of a full episode before updating the task belief; 2) they typically require numerous samples to estimate the probability distribution of the tabular-based observation model, which could be expensive and even infeasible to learn and maintain, especially using the state transition sample as the signal; and 3) they need to apply a fixed set of policies on all source tasks to obtain the tabular observation model in an offline manner, impeding the applicability to real-world continual learning settings.

To address the above limitations, we propose a scalable observation model for efficient inference on the task belief, and further extend our method to continual learning settings. First, we employ the state transition sample (s, a, r, s') as the observation signal that reveals more task information since the state transition function $\mathcal{P}(s', r|s, a)$ completely characterizes the task's dynamics. Then, we use only a small number of samples to fit the state transition functions of source tasks, which are utilized to compute the scalable observation model that can generalize to any signals observed in the target task. In particular, we adopt two typical approaches, the non-parametric Gaussian process (GP) and the parametric neural network (NN), to estimate these functions, while in principle any distribution matching technique or probabilistic model can be adopted for this estimation. GP exhibits better sample efficiency and uncertainty measurements on the predictions, while NN can scale to extremely high-dimensional tasks. Finally, we extend the offline-mode BPR to continual learning settings by expanding the scalable observation model in a plug-and-play fashion when incorporating new source policies. Experimental results show that our method achieves more efficient policy reuse and accelerates the convergence towards the best policy, as well as realizing effective continual learning performance and avoiding negative transfer.

In summary, our main contributions are threefold:

1. We employ the state transition sample as the observation signal and propose a scalable observation model to facilitate efficient policy reuse.
2. We extend the offline BPR to continual learning settings to avoid negative transfer and realize better applicability to real-world applications.
3. We perform extensive experiments to demonstrate that our method enables more efficient policy reuse and effective continual learning performance.

The remainder of the paper is organized as follows. Section 2 introduces the background including preliminaries of BPR and the related work. Section 3 presents our method in detail. Section 4 shows the experimentation, and Section 5 presents concluding remarks and future work.

2 Background

2.1 Preliminaries of BPR

BPR provides an efficient framework for an agent to perform well by selecting the most appropriate policy from the policy library Π to reuse when facing a target task. Formally, a task $\tau \in \mathcal{T}$ is defined as an MDP, and a policy $\pi \in \Pi$ is the optimal or nearly-optimal function, which outputs an appropriate action a given state s . Then, the return or utility is defined as the accumulated discounted reward $U = \sum_{i=1}^M \gamma^i r_i$, which is received from interacting with the environment under the guidance of policy π over an episode of M steps, where r_i is the instantaneous reward, and γ is the discount factor. BPR uses an observation model $P(\sigma|\tau, \pi)$, which is a probability distribution over the observation signal $\sigma \in \Sigma$, to describe possible results when policy π behaves on task τ . The belief model $\beta(\mathcal{T})$, which is a probability distribution over \mathcal{T} , describes the similarity between the new task τ_0 and the source tasks \mathcal{T} . BPR initializes the belief model $\beta^0(\mathcal{T})$ with a prior probability and update it based on the observation model and the observation signal by using Bayes' rule:

$$\beta^t(\tau) = \frac{P(\sigma^t|\tau, \pi^t) \beta^{t-1}(\tau)}{\sum_{\tau' \in \mathcal{T}} P(\sigma^t|\tau', \pi^t) \beta^{t-1}(\tau')}. \quad (1)$$

The observation signal $\sigma \in \Sigma$ can be any information correlated with the performance of a policy, and the episodic return U is the most commonly used signal. The choice of reusing policies is very crucial for each learning episode in BPR. To trade-off between exploration and exploitation, BPR uses the probability of expected improvement based on the task belief to select policies. It reuses the most potential policy $\hat{\pi}$ in the policy library Π by maximizing the expectation utility as

$$\hat{\pi} = \arg \max_{\pi \in \Pi} \sum_{\tau \in \mathcal{T}} \beta(\tau) \int_{U \in R} UP(U|\tau, \pi) dU, \quad (2)$$

where $P(U|\tau, \pi)$ is the performance model, a probability distribution over the utility U that describes how policy π behaves on the task τ .

2.2 Related Work

Knowledge transfer has received increasing attention recently and a wide variety of methods have been studied in the RL community [13, 27]. Lazaric et al. [28] transferred the state transition samples from the source to the target task by calculating the compliance (similarity) between tasks using the Bayes theorem. Brys et al. [21] provided an inter-task mapping based on state spaces to measure the similarity between two tasks, and transferred the value functions using reward shaping. Song et al. [29] transferred the value functions by measuring the distance between the source and the target tasks based on the expected models of the MDPs. Larocche and Barlier [30] estimated the reward function of the target task by reusing the experience instances of a source task. However, transfer methods based on value functions or samples usually rely on well-estimated models of the MDPs or some prior knowledge of the target task for similarity measurement, which leads to high computational complexity and could be infeasible to transfer in practice.

Instead, the other kind of approaches attempts to directly transfer policies learned in source tasks, which eliminates the requirement on the prior knowledge of the target task or the assumed models of the MDPs. Fernández et al. [31] proposed probabilistic policy reuse that transfers source policies to bias the agent’s exploration strategy in the target task. Li and Zhang [32] developed an online method of optimally selecting source policies by formulating it as a multi-armed bandit (MAB) problem. Li et al. [33] proposed a context-aware multi-policy reuse approach by employing the option framework to select the most appropriate source policy according to some contexts (e.g., a subset of states). Yang et al. [34] formulated the multi-policy transfer as an option learning problem, which serves as a complementary optimization objective of policy learning in the target task. These policy reuse approaches focus on facilitating learning the optimal policy for the target task, other than a quick response to an unknown task or rapid convergence of the target policy. Nevertheless, it is often required for RL to act online and respond quickly, in terms of rapid convergence, to novel tasks in real-world scenarios such as applications involving interactions with humans.

Rosman et al. [22] contributed BPR to quickly select source policies from an offline library using the Bayesian inference based on some observation signals and a trained observation model. BPR prefers to quickly select a pre-learned policy from a fixed library, which does not guarantee that the appropriate policy will be learned. Especially when the agent is faced with new unknown tasks, it may even result in negative transfer [35]. Further, BPR is successfully applied to handle non-stationary opponents in multi-agent systems. Hernandez-Leal et al. [23] proposed an extension, BPR+, to enable online learning of new models when the learning agent detects that the current policies are not performing optimally. Zheng et al. [25, 36] proposed deep BPR+ by extending BPR+ with a neural network. A rectified belief model using the neural network approximator is introduced to achieve accurate policy detection, and a distilled policy network is proposed as the policy library to store and reuse policies efficiently. Gao et al. [26] learned how to play with unknown opponents in bilateral negotiation games based on deep BPR+.

In contrast to the family of BPR algorithms, we use more informative observation signals such as the state transition sample, and we propose a scalable observation model to efficiently update the task belief. Although BPR+ algorithms can incorporate new models online, they still need to retrain the observation model in an offline manner when adding a new source policy into the library. Instead, our scalable observation model allows us to extend our method to continual learning settings conveniently in a truly online manner.

3 Our Method

In this section, we propose an improved BPR method that aims at more efficient policy transfer in DRL. First, we formulate the scalable observation model by fitting the state transition function from limited samples. Next, we describe in detail how to use GP and NN to estimate the observation model. Then, we extend BPR from the conventional offline mode to the continual learning setting, which can be established naturally using the scalable observation model. Finally, we present the detailed algorithm.

3.1 Scalable Observation Model

In general, BPR maintains an observation model from some observation signals to update a task similarity measure, i.e., a belief, over source tasks for positive policy reuse. Naturally, the choice of the observation signal is crucial, since it determines the granularity of the policy selection frequency and the effectiveness of the policy reuse. The most widely used observation signal in BPR is the episodic return U when fully executing an associated policy. However, using the episodic return as the observation signal has two weaknesses. One is that we must wait until the end of a full episode to obtain the signal. Some applications have very long episodes, so that delaying observing the signal

until the end of the episode is too slow. The other is that the episodic return is only a scalar that contains limited information. For example, two policies with large differences may receive similar episodic returns in the same task, or one policy can also obtain similar episodic returns in two tasks with large differences. Instead, we use the state transition sample (s, a, r, s') as the observation signal, which is supposed to reveal more task information since the state transition function $\mathcal{P}(s', r|s, a)$ completely characterizes the task's dynamics.

Suppose that we have n source tasks, and we train one source policy in each task. The observation signal could be accrued by the agent by storing the history of all state transition samples encountered during the execution of all n source policies in all n source tasks. The observation model $P(\sigma|\tau, \pi)$, in this case, is a tabular-based empirical estimate of the expected state transition function of the MDPs, which could be expensive and even infeasible to learn and maintain. It requires a large amount of state transition samples to estimate the probability distribution of the observation model, and will encounter the ‘‘curse of dimensionality’’ in large or continuous state-action spaces. Additionally, this may not generalize well, especially in cases with sparse sampling. When encountering a new sample that has not been recorded by the observation model, the Bayesian update of the task belief can easily be inaccurate in the policy reuse phase. Since the performance of BPR highly depends on the inference of the task belief, a scalable approach is necessary for building the observation model using limited state transition samples as the signal.

To address the above challenges, we propose a scalable observation model based on fitting the state transition functions of sources tasks $\mathcal{P}_j(s', r|s, a)$ from a small number of state transition samples $\mathcal{D}_j = \{(s_i^j, a_i^j, r_i^j, s'^j)\}_{i=1}^{N_j}$, where N_j is the number of samples in the j -th source task. For the convenience of expression, we denote the input and output of this supervised learning instance of fitting the state transition function as $x = (s, a)$ and $y = (r, s')$. Assume that we have learned the state transition functions of the n source tasks as $\{\mathcal{P}_j(y^j|x^j)\}_{j=1}^n$. Then, in the target task, we obtain the observation signal, i.e., a couple of state transition samples $\sigma^t = \{(x_i^0, y_i^0)\}_{i=1}^{N_0}$, by applying a selected policy π_t on the target task, where N_0 is the number of samples in the target task. The observation model $P(\sigma|\tau, \pi)$ can be naturally constructed using the fitted task dynamics as

$$P(\sigma^t|\tau_j, \pi_t) = \prod_{i=1}^{N_0} \mathcal{P}_j(y_i^0|x_i^0), \quad j = 1, \dots, n. \quad (3)$$

Intuitively, $\mathcal{P}_j(y_i^0|x_i^0)$ indicates the likelihood of the learned task dynamics \mathcal{P}_j fitting the sample (x_i^0, y_i^0) , or the degree of samples in the target task τ_0 resembling those in the source task τ_j . We only need to store a small number of samples to learn state transition functions of source tasks, which are utilized to compute the scalable observation model that can generalize to any signals observed in the target task.

3.2 Estimation of Observation Model

Since $\{\mathcal{P}_j\}_{j=1}^n$ are unknown, we only have access to an estimation of the observation model in (3). To obtain an approximation of the unknown densities, we employ two typical supervised learning approaches, the non-parametric GP [37] and the parametric NN [38], to fit the state transition function for each source task. These two methods are suitable for different situations with respective advantages.

First, we adopt GP due to its sample efficiency and the ability to provide uncertainty measurements on the predictions. GP is a non-parametric, Bayesian approach to regression that has been successfully adopted in many existing works with continuous state-action spaces [39–42]. Given a test point x_* , the j -th GP returns a Gaussian distribution over the output's mean, i.e., $\hat{y}_* \sim \mathcal{N}(\mu_{GP_j}(x_*), \text{cov}_{GP_j}(x_*))$, as

$$\begin{aligned} \mu_{GP_j}(x_*) &= \kappa_{*j} (\kappa_{jj} + \varepsilon^2 I)^{-1} Y_j, \\ \text{cov}_{GP_j}(x_*) &= \kappa_{**} - \kappa_{*j} (\kappa_{jj} + \varepsilon^2 I)^{-1} \kappa_{j*}, \end{aligned} \quad (4)$$

where (X_j, Y_j) are the training samples $\{(x_i^j, y_i^j)\}_{i=1}^{N_j}$ from the j -th source task, and κ is the kernel function such that $\kappa_{jj} = \kappa(X_j, X_j)$, $\kappa_{*j} = \kappa(x_*, X_j)$, $\kappa_{j*} = \kappa(X_j, x_*)$, $\kappa_{**} = \kappa(x_*, x_*)$. The most commonly used kernel function is the gaussian kernel, also known as the radial basis function (RBF):

$$\kappa(x, x') = \delta^2 \exp\left(-\frac{\|x - x'\|_2^2}{2l^2}\right), \quad (5)$$

where δ and l are the hyper-parameters of the RBF kernel, representing its signal variance and characteristic length scale. For more commonly used kernels, please refer to [37]. Considering each sample as an independent Gaussian distribution, the observation model in (3) can be re-arranged using the n fitted GPs $\{GP_j\}_{j=1}^n$ as

$$P(\sigma^t|\tau_j, \pi_t) = \prod_{i=1}^{N_0} \mathcal{N}(y_i^0; \mu_j(x_i^0), \text{cov}_j(x_i^0) + \varepsilon_{GP}^2), \quad (6)$$

where μ_j and cov_j denote μ_{GP_j} and cov_{GP_j} for simplicity, and ε_{GP}^2 is a constant additional variance of the Gaussian distribution, which is used to enhance generalization of GP.

Second, we adopt NN as another technique to fit the state transition function since it can scale to extremely high-dimensional problems. Having been widely investigated in supervised learning tasks, NN can extract useful information from very large data sets to build extremely complex models. Naturally, we parameterize the state transition function of a given source task as

$$\hat{Y}_j = g_{\vartheta_j}(X_j), \quad (7)$$

where $g_{\vartheta_j}(\cdot)$ is a neural network parameterized by weights ϑ_j , and \hat{Y}_j is the predicted output of the network. Each neural network is trained in a supervised learning way to minimize the loss function, e.g., the mean squared error (MSE), as

$$\mathcal{L}(\vartheta_j) = (Y_j - \hat{Y}_j)^2. \quad (8)$$

With the n fitted NNs, the observation model in (3) represents each sample as an independent Gaussian distribution, such that:

$$P(\sigma^t | \tau_j, \pi_t) = \prod_{i=1}^{N_0} \mathcal{N}(y_i^0; g_{\vartheta_j}(x_i^0), \varepsilon_{NN}^2), \quad (9)$$

where the preset constant ε_{NN}^2 is the variance of the Gaussian distribution.

For the sake of simplicity, let $f_j(x_i^0)$ and ξ_j^2 denote the mean and variance of the Gaussian distribution in the observation model, respectively. Then, we can obtain a uniform formation for the observation models in (6) and (9) as

$$P(\sigma^t | \tau_j, \pi_t) = \prod_{i=1}^{N_0} \mathcal{N}(y_i^0; f_j(x_i^0), \xi_j^2), \quad j = 1, \dots, n. \quad (10)$$

With the estimated observation model, the task belief β^t in (1) can be efficiently updated using the Bayes' rule as

$$\beta^t(\tau_j) = \frac{\prod_{i=1}^{N_0} \mathcal{N}(y_i^0; f_j(x_i^0), \xi_j^2) \beta^{t-1}(\tau_j)}{\sum_{j'=1}^n \prod_{i=1}^{N_0} \mathcal{N}(y_i^0; f_{j'}(x_i^0), \xi_{j'}^2) \beta^{t-1}(\tau_{j'})}. \quad (11)$$

3.3 Extension to Continual Learning

The conventional BPR algorithm is performed in an *offline* manner. It has to acquire a collection of pre-learned behaviors in advance, and also needs to apply a fixed set of policies on all source tasks to obtain a tabular-based observation model offline. Nevertheless, when encountering a new task, it is likely that none of the policies in the library is suitable, which leads to negative transfer. Although the BPR+ algorithms can incorporate new models online, when adding a new source policy into the library, they still need to re-estimate the observation model by applying all source policies on the new task and applying the new policy on all tasks. This can be a big barrier to the practicality of the algorithm due to the expensive and inefficient update of the observation model. Moreover, different from the learned policies, the source tasks may be inaccessible in the new learning process of the target task, in which case the observation model is infeasible to update.

To achieve artificial general intelligence, RL agents should constantly build more complex skills and scaffold their knowledge about the world in a *continual learning* manner. In the paper, we extend our method to the continual learning setting such that in the policy reuse phase, the learning agent can consult the stored library first, and either retrieve the most suitable policy from the library or expand a new policy into the library. When incorporating a new policy, we only need another GP or NN to fit the state transition function of the corresponding new source task \mathcal{P}_{n+1} using a small number of samples from that task, independent of the policies and fitted GPs or NNs from the existing source tasks. The proposed observation model in (10) is naturally scalable to the continual expansion of a new source task in a plug-and-play fashion as

$$P(\sigma^t | \tau_{n+1}, \pi_t) = \prod_{i=1}^{N_0} \mathcal{N}(y_i^0; f_{n+1}(x_i^0), \xi_{n+1}^2). \quad (12)$$

Note that the conventional BPR also maintains a performance model, i.e., a distribution of returns from each policy on the source tasks, which is utilized together with the task belief to select the most appropriate policy for reusing. As we observe the state transition function that completely characterizes the task's dynamics, the scalable observation model is informative to capture the task similarity effectively. We can merely rely on the task belief in (11) to choose reuse policies, and hence we abandon the use of the performance model for better applicability in the continual learning setting.

Algorithm 1: Efficient BPR with Scalable Observation Model

Input: Source task set \mathcal{T} ,
source policy library Π and GPs/NNs,
number of episodes K ,
the maximum number of steps M .

```

1 Initialize belief  $\beta^0(\mathcal{T})$  with a uniform distribution
2 if execute a reuse phase then
3   while episode  $\leq K$  do
4     while step  $\leq M$  & not reaching the goal do
5       Select a policy  $\pi^t \in \Pi$  based on  $\beta^{t-1}$ 
6       Apply  $\pi^t$  on target task  $\tau_0$  and receive observation signal  $\sigma^t$ 
7       Estimate  $P(\sigma^t|\mathcal{T}, \pi^t)$  in (10) by applying  $\sigma^t$  on source GPs
8       Update task belief  $\beta^t$  in (11) using the estimated  $P(\sigma^t|\mathcal{T}, \pi^t)$ 
9     end
10    if a sufficiently different task is detected then
11      Switch to the learning phase
12    end
13 else if execute a learning phase then
14   Learn a new policy  $\pi_0$  and fit a new GP/NN for  $\tau_0$ 
15   Expand  $\pi_0$  as  $\pi_{n+1}$  into the library
16   Switch to the reuse phase
17 end

```

3.4 Algorithm

Based on the above statements, we present the general form of our method in Algorithm 1. It mainly consists of two phases: the reuse phase that selects the most appropriate policy from the library in Lines 3-12, and the learning phase that expands a new optimal policy into the library in Lines 13-17.

First, the policy reuse phase is performed when facing the target task. At update step t (the step size is N_0), the agent selects a reuse policy π^t from the library $\{\pi_j\}_{j=1}^n$ according to the task belief β^{t-1} , and receives the observation signal σ^t after applying the selected policy π^t on the target task τ_0 . Next, the scalable observation model $P(\sigma^t|\tau_j, \pi^t)$ in (10) can be efficiently estimated by applying the obtained signal σ^t on the fitted GPs or NNs from the source tasks, which is used to update the task belief in (11). The two processes are iteratively alternated within a learning episode until the goal or the maximum number of steps is reached. At the end of the episode, we check whether the target task is sufficiently different from all source tasks according to the average return \bar{U} over k episodes. If \bar{U} is below a preset threshold, the agent will switch to the learning phase in subsequent episodes where a new optimal policy π_{n+1} is learned for the target task using any DRL algorithm. The obtained new policy π_{n+1} is expanded into the policy library, together with the target task τ_0 being extended as a new source task τ_{n+1} . Accordingly, a new GP or NN is generated to fit the dynamics of the new source task using a small number of samples collected from the learning phase. Finally, the agent switches back to the reuse phase for the next policy transfer problem.

Note that in some practical applications, we can empirically choose (s, a, r) or (s, a, s') alone as the observation signal for ease of use, in which case the output y of the task dynamics function in (3) is the reward r or the next state s' . Furthermore, N_0 determines the granularity of the policy selection frequency, in this paper, we update the policy reusing strategy every time step for better sample efficiency, i.e., $N_0 = 1$. In summary, our algorithm estimates the observation model from limited samples to realize efficient policy transfer. Meantime, using the scalable observation model, our algorithm can be easily extended to the continual learning setting, which makes it more practical in real-world scenarios.

4 Experiments

In this section, we evaluate our method on five different domains with increasing levels of complexity. Through these experiments, we aim to build problem settings that are representative of the types of transfer learning that RL agents may encounter in real-world scenarios. Our experiments are mainly divided into three parts:

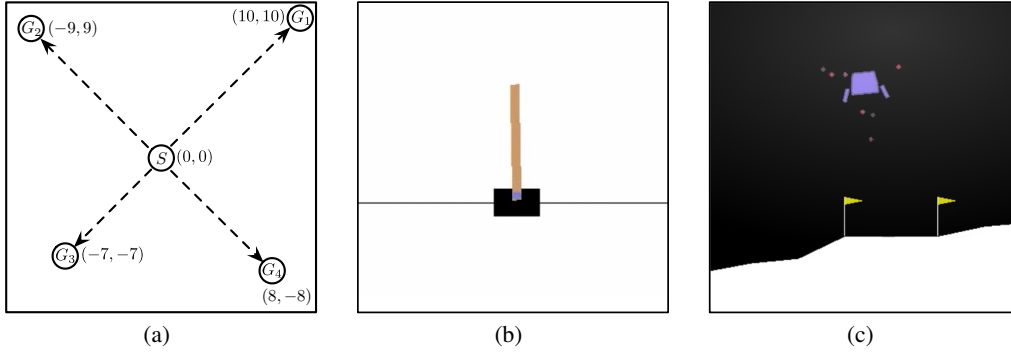


Figure 1: Three types of dynamic environments. (a) 2-D Navigation domain, S is the start point and G is the goal point. (b) CartPole domain. (c) LunarLander domain.

1. First, we implement our GP-based method in three relatively simple domains to demonstrate that it can achieve efficient policy transfer when faced with target tasks that are similar to source tasks. The results are shown in Section 4.1.
2. Second, we implement our NN-based method in two high-dimensional complex domains from MuJoCo, to verify that our method enables efficient policy transfer for more sophisticated tasks. The results are shown in Section 4.2.
3. Finally, we apply our method to all domains to prove that compared to the basic BPR algorithm, it can achieve continual learning and thus avoid negative transfer when faced with target tasks that are very different from the source tasks, as shown in Section 4.3.

In Sections 4.1 and 4.2, we compare our method to three baseline approaches for transferring policies: the family of BPR algorithms using episodic return as the observation signal [22, 36], the probabilistic Policy Reuse with DRL (PR-DRL) algorithm [20, 31, 43], and the Optimal Policy Selection with DRL (OPS-DRL) algorithm [32]. In Section 4.3, we evaluate our method in comparison to the basic BPR algorithm [22], and the settings of the BPR algorithm are consistent with those in Sections 4.1 and 4.2. For a fair comparison, we make some improvements to the baselines so that they can be directly compared with our method. The details of the three baselines are given in the Appendix.

All experimental results are averaged over 10 trials. The shaded area represents the 95% confidence interval for evaluation curves, and the standard errors are presented for numerical results. All the algorithms are implemented with Python 3.5 running on Ubuntu 16 with 48 Intel Xeon E5-2650 2.20GHz CPU processors, 193-GB RAM, and an NVIDIA Tesla GPU of 32-GB memory.

4.1 Results for Efficient Policy Transfer Based on GP

In the experiment of this section, we choose three representative types of dynamic environments, as shown in Fig. 1, and the details are as follows.

4.1.1 2-D Navigation

We first consider the navigation domain where an agent must move to a goal position in a 2-D surface, which is a continuous-state and continuous-action problem. The states are the current 2-D positions and the actions are two-dimensional vectors clipped to be in the range of $[-1, +1]$. Episodes terminate when the agent is within 0.5 of the goal or reaches the maximum number of steps $M = 100$. The reward is the negative Euclidean distance to the goal minus a control cost that is positively related to the scale of actions. We consider four source tasks, where they have the same starting points $(0, 0)$ and different goal positions as $(10, 10)$, $(-9, 9)$, $(-7, -7)$, $(8, -8)$, respectively. In this domain, tasks only differ in the reward functions. Therefore, we employ the tuple (s, a, r) as the observation signal to fit the GP and estimate the scalable observation model.

4.1.2 CartPole

We next consider a classical control problem with a continuous state and discrete action space, described in [44] and implemented in OpenAI Gym [45]. The states are four-dimensional vectors, and the actions are two discrete values

of 0 and 1. Episodes terminate when the pole falls or reaches the maximum number of steps $M = 100$. In order to encourage the agent to balance the pole, a positive reward of +1 is given at every step when the angle between the pole and vertical line is smaller than a small threshold. Otherwise, the reward is 0. The system is controlled by applying a constant force $F = 10$ newtons to the cart, and the agent can apply full force to the cart in either direction, i.e., two possible actions. We set up two source tasks by adding a constant force F' with a fixed direction on the cart. The agent needs to balance the pole with the interference of $F' = 5$ newtons in one source task, and with $F' = -5$ in the other task. In this domain, the tuple (s, a, s') is set as the observation signal to infer the most appropriate policy for the target task.

4.1.3 LunarLander

We choose a relatively complex task, the LunarLanderContinuous-v2 domain from OpenAI-Gym, which involves landing a spacecraft safely on a lunar surface. This is a high-dimensional continuous control problem with sparse reward, and is representative of real-world problems where it is considerably difficult to learn accurate dynamics. The states are eight-dimensional vectors. The actions are two-dimensional vectors clipped to be in the range of $[-1, +1]$, which are used to control the powers of the main and side engines. Episodes finish if the lander crashes or comes to rest or reaches the maximum number of steps $M = 1000$. In this case, it can take a large number of steps to reach the goal, and the reward is significantly delayed until the end of the long episode. We set up three source tasks that represent three typical scenarios by applying an additional constant power with a fixed direction on the main engine of the spacecraft. The additive powers are $(0.5, 0)$, $(-0.5, 0)$, and $(0, 0.5)$, respectively. A successful transfer agent should learn to transfer skills from the source tasks and try to avoid the potential risk of landing the spacecraft. Here, the moon surface is generated randomly in each episode, so the environmental dynamics are learned on noisy data. To solve this problem, during the experiment, we set up a constant random seed for the environment. In this setting, tasks mainly differ in the state transition functions. Therefore, we can employ the tuple (s, a, s') as the observation signal to infer the task belief.

In this experiment, we select some target tasks that are relatively close to the source tasks in each domain, which ensures that there are suitable policies for the target tasks in the policy library.

- In 2-D Navigation domain, we select twelve target tasks, and their goal positions are $(10.5, 10)$, $(10, 9.5)$, $(-8.5, 9)$, $(-9, 9.5)$, $(-6.5, -7)$, $(-7, -7.5)$, $(7.5, -8)$, $(8, -7.5)$, $(10, 10)$, $(-9, 9)$, $(-7, -7)$, $(8, -8)$.
- In CartPole domain, we select six target tasks, and their values of the additional force F' are set as 4.5, 5, 5.5, -5.5, -5, -4.5.
- In LunarLander domain, we select nine target tasks, and their value of additive powers are $(0.45, 0)$, $(-0.45, 0)$, $(0, 0.45)$, $(0.55, 0)$, $(-0.55, 0)$, $(0, 0.55)$, $(0.5, 0)$, $(-0.5, 0)$, $(0, 0.5)$.

In each experiment, the number of learning episodes in the target task, K , is set as 10, which is supposed to be sufficient for all tested methods to converge to the most appropriate policy with the highest return. The hyperparameters are set as: $\delta = 1$ and $l = 2$ for the RBF kernel of the GPR. $\varepsilon_{GP}^2 = 0.1$ for the Gaussian distribution of all test domains. And in this experiment, we use vanilla policy gradient (REINFORCE) [46, 47] and twin delayed deep deterministic policy gradient (TD3) algorithm [48] to learn optimal policies for source tasks.

We present the primary results of our GP-based method and all baseline approaches on three relatively simple experimental domains, and all the results are averaged over multiple target tasks. Fig. 2 shows the average return per learning episode, and Table 1 reports the numerical results in terms of average return over all learning episodes. BPR obtains better policy transfer performance than PR-DRL and OPS-DRL, which is supposed to benefit from leveraging the efficiency of the Bayesian inference framework. It is clear that our method achieves much more efficient policy transfer in all tasks compared to baselines. From Figs. 2-(a) and 2-(b), it is observed that the received return of our method in the first episode is nearly equal to that of the best policies for target tasks, since our method can converge to the most appropriate policy using a few steps within the first episode. In more complex domains, our method can also achieve much better jump-start performance compared to all baselines, as illustrated in Fig. 2-(c). Further, from the numerical results in Table 1, our method generally obtains the largest average return over all learning episodes in all domains. In addition, it can be observed from the statistical results that our method mostly obtains smaller confidence intervals and standard errors than the baselines. This phenomenon indicates that our method can provide more stable source task selection and knowledge transfer.

We also study how the number of state transition samples (s, a, r, s') used for fitting the GPs affects the performance of our method, i.e., identifying the relationship between the sample size and the accuracy of policy detection during the policy reuse phase in our method. We use 100, 200, 500, 1000, and 2000 samples, respectively, for fitting state transition functions using GPs in these domains to observe the performance of our method. Fig. 3 shows the average return per learning episode, and Table 2 reports the numerical results in terms of average return over all learning

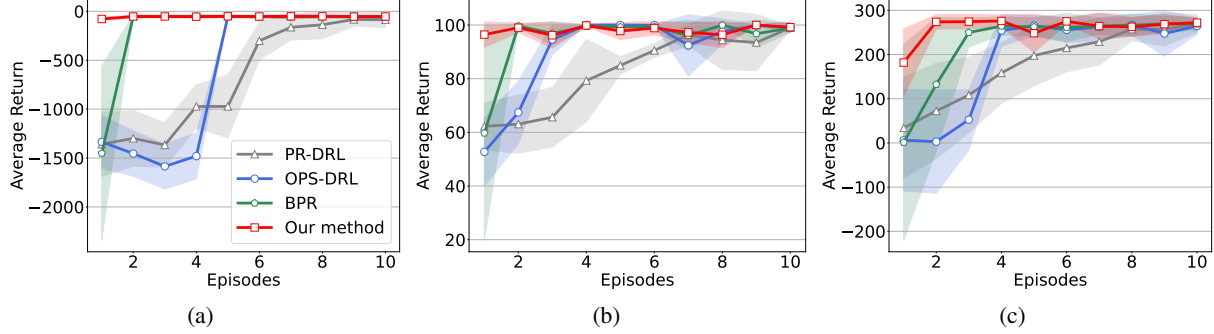


Figure 2: Average return per episode of all tested methods in: (a) 2-D Navigation; (b) CartPole; (c) LunarLander.

Table 1: Average return over all episodes of all test methods implemented in three domains.

Method	PR-DRL	OPS-DRL	BPR	Our method
2-D Navigation	-674.19 ± 581.44	-618.02 ± 709.72	-193.39 ± 505.16	-55.33 ± 16.53
CartPole	82.88 ± 16.41	90.36 ± 17.16	94.59 ± 17.46	98.08 ± 3.53
LunarLander	179.88 ± 105.79	187.87 ± 126.69	224.09 ± 121.28	259.75 ± 41.98

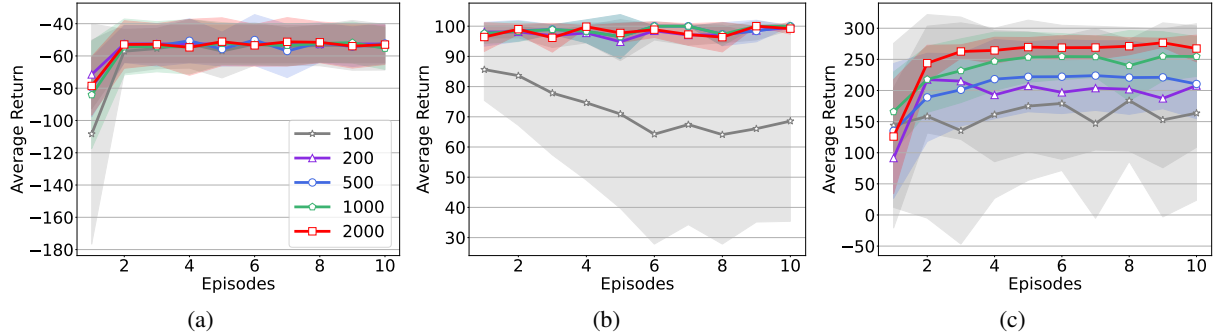


Figure 3: Average return per episode of different sample sizes used for GPs in: (a) 2-D Navigation; (b) CartPole; (c) LunarLander.

Table 2: Average return over all episodes of different sample sizes used for GPs in three domains.

Sample size	100	200	500	1000	2000
2-D Navigation	-59.87 ± 30.06	-54.46 ± 14.09	-55.75 ± 16.01	-56.53 ± 19.33	-55.33 ± 16.53
CartPole	72.31 ± 29.62	97.65 ± 3.54	98.53 ± 3.72	98.70 ± 3.50	98.08 ± 3.53
LunarLander	186.43 ± 105.72	192.43 ± 125.87	206.37 ± 70.66	237.42 ± 53.50	251.97 ± 54.57

episodes. In all domains, our method obtains a significant performance improvement when the sample size goes from 100 to 200. Then, as the sample size continues to grow, the performance of our method is slightly improved only, and the degree of performance improvement is decreasing. Especially in the 2-D Navigation and CartPole domains, the performance of our method remains roughly the same. It demonstrates that using only a small number of samples to fit the state transition function, our method is capable of accurately estimating the scalable observation model and inferring the task belief for efficient policy transfer.

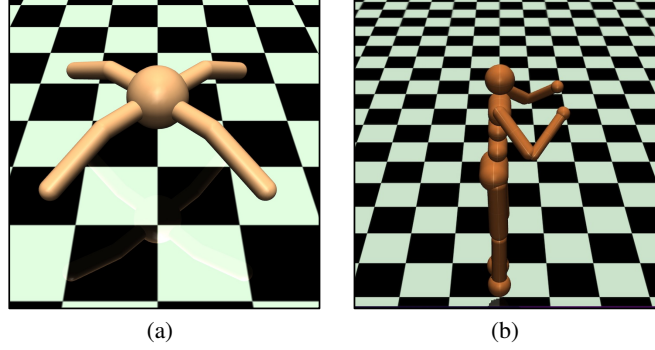


Figure 4: Two types of dynamic environments. (a) Ant-Navigation domain. (b) Humanoid-Navigation domain.

4.2 Results for Efficient Policy Transfer Based on NN

In the experiment of this section, we choose two high-dimensional dynamic environments from MuJoCo [49], as shown in Fig. 4, and the details are as follows.

4.2.1 Ant-Navigation

The first experiment consists of a variation of the Ant-v3, which makes an ant agent reach the specified 2-D positions. The states are 113-dimensional vectors, and the actions are 8-dimensional vectors clipped to be in the range of $[-1, +1]$. In our experiment, the ant agent only needs to be within 0.2 of the goal from the starting point or reach the maximum number of steps $M = 100$ regardless of speed. The reward consists of three parts: the negative Euclidean distance to the goal, a control cost that is positively related to the scale of actions, and a contact cost that is positively related to the scale of contact forces. We set up four source tasks with different goal positions and gear on the legs of the ant agent, where the gear is used to specify 3D force and torque axes by scaling the length of the actuator. The goal positions are $(1, 1)$, $(-1, 1)$, $(-1, -1)$, $(1, -1)$, and the corresponding gears are 50, 100, 150, 200, respectively. When faced with target tasks similar to the source ones, we need to select the most appropriate policy from the library. To solve this problem, the tuple (s, a, r, s') is used as the observation signal.

4.2.2 Humanoid-Navigation

We design the fifth experiment to verify that our method can solve very high-dimensional problems. We adopt a variation of the Humanoid-v3, which makes a humanoid agent reach the specified 2-D position. It is very challenging to solve this high-dimensional problem with a continuous state-action space. The states are 378-dimensional vectors, and the actions are 17-dimensional vectors clipped to be in the range of $[-0.4, +0.4]$. In this experiment, the humanoid agent will end the episode when it reaches the specified range of the goal or the maximum number of steps $M = 1000$, or it falls. The reward contains four parts: the negative Euclidean distance to the goal, an alive bonus when the z -coordinate of the agent is in the specified range, a large bonus when the agent reaches its goal, and a control and impact cost. We set up four source tasks where the goal positions are $(0.6, 0.6)$, $(-0.55, 0.55)$, $(0.5, -0.5)$ and $(-0.45, -0.45)$, and the corresponding specified ranges are 0.4, 0.35, 0.3, 0.25, respectively. To solve this problem, we use the tuple (s, a, r) as the observation signal.

Analogous to Section 4.1, we select some target tasks that are relatively close to the source tasks in each domain.

- In Ant-Navigation domain, we select twelve target tasks, and their goal positions and gears are $(1.1, 1.1, 60)$, $(0.9, 0.9, 40)$, $(1.1, -1.1, 90)$, $(0.9, -0.9, 110)$, $(-1.1, 1.1, 160)$, $(-0.9, 0.9, 140)$, $(-1.1, -1.1, 190)$, $(-0.9, -0.9, 210)$, $(1, 1, 50)$, $(1, -1, 100)$, $(-1, 1, 150)$, $(-1, -1, 200)$.
- In Humanoid-Navigation domain, we select twelve target tasks, and their goal positions and specified ranges are $(0.55, 0.55, 0.4)$, $(0.65, 0.65, 0.4)$, $(-0.5, 0.5, 0.35)$, $(-0.6, 0.6, 0.35)$, $(0.45, -0.45, 0.3)$, $(0.55, -0.55, 0.35)$, $(-0.5, -0.5, 0.25)$, $(-0.4, -0.4, 0.25)$, $(0.6, 0.6, 0.4)$, $(-0.55, 0.55, 0.35)$, $(0.5, -0.5, 0.3)$, $(-0.45, -0.45, 0.25)$.

In this experiment, the number of learning episodes in the target task, K , is set as 10. The hyper-parameters are set as: $\varepsilon_{NN}^2 = 0.1$ for the Ant-Navigation domain and $\varepsilon_{NN}^2 = 1$ for the Humanoid-Navigation domain. To solve complex

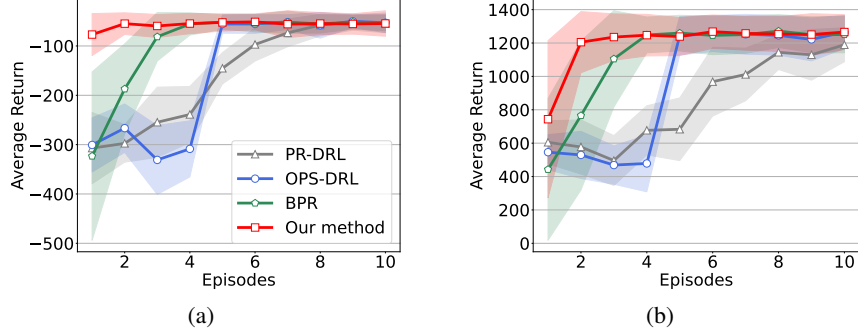


Figure 5: Average return per episode of all tested methods in two domains. (a) Ant-Navigation. (b) Humanoid-Navigation.

Table 3: Average return over all episodes of all test methods implemented in two domains.

Method	PR-DRL	OPS-DRL	BPR	Our method
Ant-Navigation	-157.79 ± 109.36	-153.05 ± 128.53	-96.46 ± 107.31	-56.94 ± 25.78
Humanoid-Navigation	848.15 ± 295.14	950.91 ± 384.62	1108.84 ± 354.02	1196.59 ± 243.20

problems, we use the twin delayed deep deterministic policy gradient (TD3) algorithm [48] to learn optimal policies for source tasks.

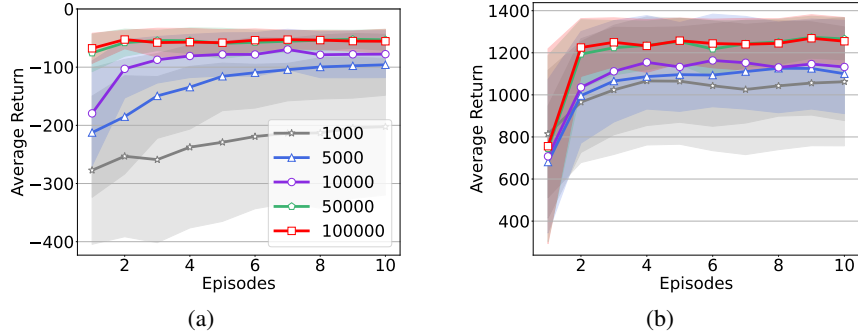


Figure 6: Average return per episode of different sample sizes used for NNs in: (a) Ant-Navigation; (b) Humanoid-Navigation.

Table 4: Average return over all episodes of different sample sizes used for NNs in two domains.

Sample size	1000	5000	100000	50000	100000
Ant-Navigation	-230.84 ± 132.05	-130.40 ± 81.34	-91.06 ± 56.40	-57.28 ± 22.61	-56.34 ± 20.95
Humanoid-Navigation	1016.49 ± 311.26	1048.26 ± 273.24	1086.82 ± 276.53	1190.30 ± 234.84	1197.40 ± 236.57

We present the primary results of our NN-based method and all baseline methods on two complex experimental domains, and all the results are averaged over multiple target tasks. Fig. 5 shows the average return per learning episode, and Table 3 reports the numerical results in terms of average return over all learning episodes. BPR obtains better policy transfer performance than PR-DRL and OPS-DRL, and our method achieves much more efficient policy transfer in all tasks compared to BPR. In domains with high-dimensional, our method can also achieve much better jump-start performance compared to all baselines, as illustrated in Figs. 5-(a) and 5-(b). Further, from the numerical results in Table 1, our method generally obtains the largest average return over all learning episodes in all domains. In addition, it can be observed from the statistical results that our method mostly obtains smaller confidence intervals and

Table 5: The final received returns implemented in all domains with continual learning settings.

Domain	2-D Navigation	CartPole	LunarLander	Ant-Navigation	Humanoid-Navigation
BPR	-895.15 ± 292.44	34.0 ± 10.34	-33.25 ± 87.71	-288.05 ± 62.82	343.61 ± 110.79
Our method	-39.82 ± 5.39	96.44 ± 2.90	-24.96 ± 5.29	-70.08 ± 11.30	1347.82 ± 89.98

standard errors than the baselines. This phenomenon indicates that our method can provide more stable source task selection and knowledge transfer in high-dimensional domains.

Moreover, we study how the number of state transition samples (s, a, r, s') used for fitting the NNs affects the performance of our method. We use 1000, 5000, 10000, 50000, and 100000 samples, respectively, for fitting the state transition functions using NNs in all domains to observe the performance of our method. Fig. 6 shows the average return per learning episode, and Table 4 reports the numerical results in terms of average return over all learning episodes. In all domains, as the sample size continues to grow, the performance of our method is improved, but the degree of performance improvement is decreasing. When the sample size reaches 50000, the performance is almost optimal. It demonstrates that using the limited number of samples to fit the state transition function, our method based on NN is capable of accurately estimating the scalable observation model and inferring the task belief for efficient policy transfer.

Overall, it is verified that our method achieves more accurate inference of the task belief and converges more quickly to the most appropriate policy for the target task. Using the scalable observation model with more informative observation signals, our method can efficiently update the task belief and achieve better performance compared to all baselines in all experimental domains.

4.3 Results for Continual Learning

In this experiment, we evaluate our method and the baseline approach in continual learning settings where the agent is faced with a new unknown target task that largely differs from any of the source tasks.

- In 2-D Navigation domain, we select four target tasks, and their goal positions are $(0, 10)$, $(0, -9)$, $(-8, 0)$, $(9, 0)$.
- In CartPole domain, we select two target tasks, and their values of the additional force F' are 8, -8 .
- In LunarLander domain, we select two target tasks, and their value of additive powers are $(0.5, 0.5)$, $(-0.5, 0.5)$.
- In Ant-Navigation domain, we select four target tasks, and their goal positions and gears are $(1, 0, 50)$, $(-0.9, 0, 100)$, $(0, -0.8, 150)$, $(0, 0.9, 200)$.
- In Humanoid-Navigation domain, we select four target tasks, and their goal positions and specified ranges are $(0.2, 0.7, 0.3)$, $(-0.65, 0.2, 0.3)$, $(0.25, -0.6, 0.3)$, $(0, -0.8, 0.3)$.

Different from the previous settings, our method is required to learn a new policy for the target task in an online fashion, other than selecting an existing source policy from the offline library, when a sufficiently different target task is detected. In this setting, we compare our method to the BPR and we deploy the agents to some target tasks that are not close to the source ones, and the final received returns are shown in Table 5. It is observed that BPR performs worse in the five domains since it is unable to select an appropriate policy from the offline library to respond to a new unknown task. In contrast, our method can learn a new optimal policy for the target task by expanding the source library in a continual learning manner. In the policy reuse phase, our method can detect the unknown tasks according to the received return, and switch to the learning phase to learn a new optimal policy for the target task, thus effectively avoiding negative transfer.

5 Conclusions and Future Work

In the paper, we proposed a general improved BPR framework to implement more efficient policy transfer in DRL. The scalable observation model was introduced by fitting state transition functions of source tasks using the non-parametric GP or parametric NN, which achieves more accurate policy detection and faster policy convergence with informative and instantaneous observation signals. GP is merited for its sample efficiency and the ability to provide uncertainty measurements on the predictions, while NN is preferred for extremely high-dimensional tasks. Moreover, we extended our method to continual learning settings conveniently in a plug-and-play fashion to avoid negative transfer.

While we use GP and NN to estimate the observation model, our method is a general framework and can be easily combined with any distribution matching technique or probabilistic model. Thus, a potential direction for future work is to use more powerful techniques to estimate the observation model, such as Bayesian neural networks. Alternatively, a potential solution is to use the return distribution of distributional RL approaches to avoid introducing any additional models. Another direction is to improve the settings of continuous learning, for example, using policy distillation to speed up the learning process for unknown tasks.

References

- [1] R. S. Sutton and A. G. Barto, *Reinforcement Learning: An Introduction*, 2nd ed. MIT Press, 2018.
- [2] Z. Zhang, D. Wang, and J. Gao, “Learning automata-based multiagent reinforcement learning for optimization of cooperative tasks,” *IEEE Transactions on Neural Networks and Learning Systems*, vol. 32, no. 10, pp. 4639–4652, 2020.
- [3] H. Li, Q. Zhang, and D. Zhao, “Deep reinforcement learning-based automatic exploration for navigation in unknown environment,” *IEEE Transactions on Neural Networks and Learning Systems*, vol. 31, no. 6, pp. 2064–2076, 2020.
- [4] O. Vinyals, I. Babuschkin, W. M. Czarnecki, M. Mathieu, A. Dudzik, J. Chung, D. H. Choi, R. Powell, T. Ewalds, P. Georgiev *et al.*, “Grandmaster level in StarCraft II using multi-agent reinforcement learning,” *Nature*, vol. 575, no. 7782, pp. 350–354, 2019.
- [5] D. Silver, J. Schrittwieser, K. Simonyan, I. Antonoglou, A. Huang, A. Guez, T. Hubert, L. Baker, M. Lai, A. Bolton *et al.*, “Mastering the game of Go without human knowledge,” *Nature*, vol. 550, no. 7676, pp. 354–359, 2017.
- [6] J. Hwangbo, J. Lee, A. Dosovitskiy, D. Bellicoso, V. Tsounis, V. Koltun, and M. Hutter, “Learning agile and dynamic motor skills for legged robots,” *Science Robotics*, vol. 4, no. 26, 2019.
- [7] C. Huang, R. Zhang, M. Ouyang, P. Wei, J. Lin, J. Su, and L. Lin, “Deductive reinforcement learning for visual autonomous urban driving navigation,” *IEEE Transactions on Neural Networks and Learning Systems*, vol. 32, no. 12, pp. 5379–5391, 2021.
- [8] J.-A. Li, D. Dong, Z. Wei, Y. Liu, Y. Pan, F. Nori, and X. Zhang, “Quantum reinforcement learning during human decision-making,” *Nature Human Behaviour*, vol. 4, pp. 294–307, 2020.
- [9] P. Henderson, R. Islam, P. Bachman, J. Pineau, D. Precup, and D. Meger, “Deep reinforcement learning that matters,” in *Proceedings of AAAI Conference on Artificial Intelligence*, vol. 32, no. 1, 2018, pp. 3207–3214.
- [10] S. Majumdar, S. Khadka, S. Miret, S. Mcaleer, and K. Tumer, “Evolutionary reinforcement learning for sample-efficient multiagent coordination,” in *Proceedings of International Conference on Machine Learning*, vol. 119, 2020, pp. 6651–6660.
- [11] D. Yarats, A. Zhang, I. Kostrikov, B. Amos, J. Pineau, and R. Fergus, “Improving sample efficiency in model-free reinforcement learning from images,” in *Proceedings of AAAI Conference on Artificial Intelligence*, vol. 35, no. 12, 2021, pp. 10 674–10 681.
- [12] E. Mitchell, R. Rafailov, X. B. Peng, S. Levine, and C. Finn, “Offline meta-reinforcement learning with advantage weighting,” in *Proceedings of International Conference on Machine Learning*, vol. 139, 2021, pp. 7780–7791.
- [13] M. E. Taylor and P. Stone, “Transfer learning for reinforcement learning domains: A survey,” *Journal of Machine Learning Research*, vol. 10, no. 7, 2009.
- [14] Z. Xu, K. Wu, Z. Che, J. Tang, and J. Ye, “Knowledge transfer in multi-task deep reinforcement learning for continuous control,” in *Proceedings of Advances in Neural Information Processing Systems*, vol. 33, 2020, pp. 15 146–15 155.
- [15] M. Abdolshah, H. Le, T. K. George, S. Gupta, S. Rana, and S. Venkatesh, “A new representation of successor features for transfer across dissimilar environments,” in *Proceedings of International Conference on Machine Learning*, vol. 139, 2021, pp. 1–9.
- [16] J. Pan, X. Wang, Y. Cheng, and Q. Yu, “Multisource transfer double DQN based on actor learning,” *IEEE Transactions on Neural Networks and Learning Systems*, vol. 29, no. 6, pp. 2227–2238, 2018.
- [17] A. Gupta, C. Devin, Y. Liu, P. Abbeel, and S. Levine, “Learning invariant feature spaces to transfer skills with reinforcement learning,” in *Proceedings of International Conference on Learning Representations*, 2017.
- [18] E. Parisotto, J. L. Ba, and R. Salakhutdinov, “Actor-mimic: Deep multitask and transfer reinforcement learning,” in *Proceedings of International Conference on Learning Representations*, 2016.
- [19] J. Yang, B. Petersen, H. Zha, and D. Faissol, “Single episode policy transfer in reinforcement learning,” in *Proceedings of International Conference on Learning Representations*, 2020.
- [20] A. Barreto, W. Dabney, R. Munos, J. J. Hunt, T. Schaul, H. van Hasselt, and D. Silver, “Successor features for transfer in reinforcement learning,” in *Proceedings of Advances in Neural Information Processing Systems*, 2017, p. 4058–4068.
- [21] T. Brys, A. Harutyunyan, M. E. Taylor, and A. Nowé, “Policy transfer using reward shaping,” in *Proceedings of International Conference on Autonomous Agents and Multiagent Systems*, 2015, pp. 181–188.
- [22] B. Rosman, M. Hawasly, and S. Ramamoorthy, “Bayesian policy reuse,” *Machine Learning*, vol. 104, no. 1, pp. 99–127, 2016.

- [23] P. Hernandez-Leal, B. Rosman, M. E. Taylor, L. E. Sucar, and E. Munoz de Cote, “A Bayesian approach for learning and tracking switching, non-stationary opponents,” in *Proceedings of International Conference on Autonomous Agents and Multiagent Systems*, 2016, pp. 1315–1316.
- [24] T. Yang, J. Hao, Z. Meng, C. Zhang, Y. Zheng, and Z. Zheng, “Towards efficient detection and optimal response against sophisticated opponents,” in *Proceedings of International Joint Conference on Artificial Intelligence*, 2019, pp. 623–629.
- [25] Y. Zheng, Z. Meng, J. Hao, Z. Zhang, T. Yang, and C. Fan, “A deep Bayesian policy reuse approach against non-stationary agents,” in *Proceedings of Advances in Neural Information Processing Systems*, vol. 31, 2018, pp. 962–972.
- [26] X. Gao, S. Chen, Q. Sun, Y. Zheng, and J. Hao, “A Bayesian policy reuse approach for bilateral negotiation games,” in *Proceedings of AAAI Conference on Artificial Intelligence, Workshop on Reinforcement Learning in Games*, 2022.
- [27] Y. Tao, S. Genc, J. Chung, T. Sun, and S. Mallya, “Repaint: Knowledge transfer in deep reinforcement learning,” in *Proceedings of International Conference on Machine Learning*, vol. 139, 2021, pp. 10 141–10 152.
- [28] A. Lazaric, M. Restelli, and A. Bonarini, “Transfer of samples in batch reinforcement learning,” in *Proceedings of International Conference on Machine Learning*, 2008, pp. 544–551.
- [29] J. Song, Y. Gao, H. Wang, and B. An, “Measuring the distance between finite markov decision processes,” in *Proceedings of International Conference on Autonomous Agents and Multiagent Systems*, 2016, pp. 468–476.
- [30] R. Larocche and M. Barlier, “Transfer reinforcement learning with shared dynamics,” in *Proceedings of AAAI Conference on Artificial Intelligence*, vol. 31, 2017, pp. 2147–2153.
- [31] F. Fernández, J. García, and M. Veloso, “Probabilistic policy reuse for inter-task transfer learning,” *Robotics and Autonomous Systems*, vol. 58, no. 7, pp. 866–871, 2010.
- [32] S. Li and C. Zhang, “An optimal online method of selecting source policies for reinforcement learning,” in *Proceedings of AAAI Conference on Artificial Intelligence*, vol. 32, no. 1, 2018, pp. 3562–3570.
- [33] S. Li, F. Gu, G. Zhu, and C. Zhang, “Context-aware policy reuse,” in *Proceedings of International Conference on Autonomous Agents and Multiagent Systems*, 2019, p. 989–997.
- [34] T. Yang, J. Hao, Z. Meng, Z. Zhang, Y. Hu, Y. Chen, C. Fan, W. Wang, W. Liu, Z. Wang, and J. Peng, “Efficient deep reinforcement learning via adaptive policy transfer,” in *Proceedings of International Joint Conference on Artificial Intelligence*, 2020, pp. 3094–3100.
- [35] S. J. Pan and Q. Yang, “A survey on transfer learning,” *IEEE Transactions on Knowledge and Data Engineering*, vol. 22, no. 10, pp. 1345–1359, 2009.
- [36] Y. Zheng, J. Hao, Z. Zhang, Z. Meng, T. Yang, Y. Li, and C. Fan, “Efficient policy detecting and reusing for non-stationarity Markov games,” *Autonomous Agents and Multi-Agent Systems*, vol. 35, no. 1, pp. 1–29, 2021.
- [37] M. Seeger, “Gaussian processes for machine learning,” *International Journal of Neural Systems*, vol. 14, no. 02, pp. 69–106, 2004.
- [38] Y. LeCun, Y. Bengio, and G. Hinton, “Deep learning,” *Nature*, vol. 521, no. 7553, pp. 436–444, 2015.
- [39] C. E. Rasmussen, M. Kuss *et al.*, “Gaussian processes in reinforcement learning,” in *Proceedings of Advances in Neural Information Processing Systems*, vol. 4, 2003.
- [40] M. Deisenroth and C. E. Rasmussen, “PILCO: A model-based and data-efficient approach to policy search,” in *Proceedings of International Conference on Machine Learning*, 2011, pp. 465–472.
- [41] F. Doshi-Velez and G. Konidaris, “Hidden parameter Markov decision processes: A semiparametric regression approach for discovering latent task parametrizations,” in *Proceedings of International Joint Conference on Artificial Intelligence*, vol. 2016, 2016, p. 1432.
- [42] F. Berkenkamp, M. Turchetta, A. P. Schoellig, and A. Krause, “Safe model-based reinforcement learning with stability guarantees,” in *Proceedings of Advances in Neural Information Processing Systems*, vol. 2, 2017, pp. 909–919.
- [43] Z. Wang, H.-X. Li, and C. Chen, “Incremental reinforcement learning in continuous spaces via policy relaxation and importance weighting,” *IEEE Transactions on Neural Networks and Learning Systems*, vol. 31, no. 6, pp. 1870–1883, 2020.
- [44] S. Geva and J. Sitte, “A cartpole experiment benchmark for trainable controllers,” *IEEE Control Systems Magazine*, vol. 13, no. 5, pp. 40–51, 1993.
- [45] G. Brockman, V. Cheung, L. Pettersson, J. Schneider, J. Schulman, J. Tang, and W. Zaremba, “OpenAI Gym,” *arXiv preprint arXiv:1606.01540*, 2016.
- [46] R. J. Williams, “Simple statistical gradient-following algorithms for connectionist reinforcement learning,” *Machine Learning*, vol. 8, no. 3, pp. 229–256, 1992.
- [47] Y. Duan, X. Chen, R. Houthoofd, J. Schulman, and P. Abbeel, “Benchmarking deep reinforcement learning for continuous control,” in *Proceedings of International Conference on Machine Learning*, 2016, pp. 1329–1338.
- [48] S. Fujimoto, H. Hoof, and D. Meger, “Addressing function approximation error in actor-critic methods,” in *Proceedings of International Conference on Machine Learning*, 2018, pp. 1587–1596.
- [49] E. Todorov, T. Erez, and Y. Tassa, “MuJoCo: A physics engine for model-based control,” in *Proceedings of IEEE/RSJ International Conference on Intelligent Robots and Systems*, 2012, pp. 5026–5033.

Appendix Baselines of BPR, PR-DRL, and OPS-DRL

A BPR

The family of BRP algorithms [22–26, 36] typically uses the episodic return as the observation signal, and needs to apply all source policies on all source tasks to estimate the tabular-based observation model in an offline manner. However, it requires a large amount of episode return samples to estimate the probability distribution of the observation model. In our experiments, for better applicability, we employ a variant of the BPR algorithms, which models the probability distribution of the observation model as a Gaussian distribution. For each task-policy pair (τ, π) , we apply the source policy π on the source τ , and repeat it one hundred times. Then, we take the mean of episode returns μ_U , and artificially choose an appropriate variance ε_U^2 . In this way, we can obtain the observation model as $P(\sigma \mid \tau, \pi) \sim \mathcal{N}(\mu_U, \varepsilon_U^2)$.

B PR-DRL

The probabilistic policy reuse algorithm [31] improves its exploration by exploiting the source policies probabilistically. It updates the probability depending on the reuse gains, which are obtained concurrently during the learning process. The original probabilistic Policy Reuse (PR) algorithm was implemented by the Q-learning, referred to as PRQ-learning, which can be applied to simple domains with a discrete state-action space only. Here, we adopt a version of PRQ-learning that builds on DRL, similar to the experimental settings in [20, 43]. Thus, the resulting approach is called PR-DRL that is directly comparable to our method. Algorithm 2 shows its pseudocode, where the initial value of the temperature parameter ν is 0, and the value of the incremental size $\Delta\nu$ is 0.05.

C OPS-DRL

The Optimal Policy Selection (OPS) algorithm [32] formulates online source policy selection as a multi-armed bandit problem and augments Q-learning with policy reuse. Analogous to the setting of PR-DRL, we adopt a version of OPS that builds on DRL and obtain another baseline approach as OPS-DRL. Note that the original OPS algorithm initializes the reuse gains of source policies by applying all the source policies on the target task. For a fair comparison, we set the initial reuse gains of source policies in the OPS-DRL as zeros. The pseudocode is shown in Algorithm 3. Moreover, PR-DRL and OPS-DRL learn a new policy for the target task while reusing source policies from the policy library. For a fair comparison with our method, we assume that the two baselines only reuse source policies without learning a new one.

Algorithm 2: PR-DRL

Input: Source policy library $\{\pi_j\}_{j=1}^n$,
 number of episodes K ,
 the maximum number of steps M .

- 1 $W_j \leftarrow 0$, the reuse gain associated with π_j ,
- 2 $V_j \leftarrow 0$, the number of times π_j is used.
- 3 Temperature parameter ν and the incremental size $\Delta\nu$
- 4 **while** $episode \leq K$ **do**
- 5 **while** $j \leq n$ **do**
- 6 $p_j \leftarrow e^{\nu \times W_j} / \sum_{j'}^n e^{\nu \times W_{j'}}$
- 7 **end**
- 8 Select the reuse policy π_j according P .
- 9 $U \leftarrow 0$
- 10 **while** $step \leq M$ & *not reaching the goal* **do**
- 11 Apply π_j on target task τ_0 and receive the reward r_t .
- 12 $U = U + \gamma^t r_t$
- 13 **end**
- 14 $W_j \leftarrow \frac{W_j \times V_j + U}{V_j + 1}$
- 15 $V_j \leftarrow V_j + 1$
- 16 $\nu = \nu + \Delta\nu$
- 17 **end**

Algorithm 3: OPS-DRL

Input: Source policy library $\{\pi_j\}_{j=1}^n$,
 number of episodes K ,
 the maximum number of steps M .

```

1  $W_j \leftarrow 0$ , the reuse gain associated with  $\pi_j$ ,
2  $V_j \leftarrow 0$ , the number of times  $\pi_j$  is used.
3 while  $episode \leq K$  do
4     Select the reuse policy  $\pi_j$  according:  $j = \arg \max_{1 \leq j \leq n} \left( W_j + \sqrt{\frac{2 \ln(\sum_{j=1}^n V_j + 1)}{V_j + 1}} \right)$ .
5      $U \leftarrow 0$ 
6     while  $step \leq M$  & not reaching the goal do
7         Apply  $\pi_j$  on target task  $\tau_0$  and receive the reward  $r_t$ .
8          $U = U + \gamma^t r_t$ 
9     end
10     $W_j \leftarrow \frac{W_j \times V_j + U}{V_j + 1}$ 
11     $V_j \leftarrow V_j + 1$ 
12 end
    
```
